Machining Science and Technology, 15:1–20
ISSN: 1091-0344 print/1532-2483 online
DOI: 10.1080/10910344.2011.557943

Taylor & Francis
Taylor & Francis Group

DYNAMIC PROPERTIES FOR MODELING AND SIMULATION OF MACHINING: EFFECT OF PEARLITE TO AUSTENITE PHASE TRANSITION ON FLOW STRESS IN AISI 1075 STEEL

Timothy J. Burns[1], Steven P. Mates[1], Richard L. Rhorer[1], Eric P. Whitenton[1], and Debasis Basak[2]
[1]*National Institute of Standards and Technology, Gaithersburg, MD, USA*
[2]*Orbital Sciences Corporation, Dulles, VA, USA*

□ *The Pulse-Heated Kolsky Bar Laboratory at the National Institute of Standards and Technology (NIST) has been developed for the measurement of dynamic properties of metals. With this system, a small sample can be pre-heated from room temperature to several hundred degrees* C *in less than a second, prior to rapid loading in compression at strain rates up to the order of* 10^4 *per second. A major focus of this research program has been on investigating the influence of the heating rate and time at temperature on the flow stress of carbon steels, for application to the modeling and simulation of high-speed machining operations. The unique pulse heating capability of the NIST Kolsky bar system enables flow stress measurements to be obtained under conditions that differ significantly from those in which the test specimens have been pre-heated to a high temperature more slowly, because there is less time for thermally activated microstructural processes such as dislocation annealing, grain growth, and solid state phase transformations to take place. New experimental results are presented on AISI 1075 pearlitic steel samples that were pulse-heated up to and beyond the austenite formation temperature of the material (723°C). The data show that the flow stress decreased by about 50% due to a phase transformation in the microstructure of the material from the stronger pearlitic phase to the weaker austenitic phase. As a result, the constitutive response behavior of the material cannot be modeled by a fixed-parameter constitutive model, like the Johnson-Cook flow stress model that is widely used in computer simulations of high-speed machining processes.*

Keywords AISI 1075 steel, high-speed machining, Johnson-Cook model, split-Hopkinson pressure bar

INTRODUCTION

Prediction of the best machining parameters for a particular process and work material continues to be a challenge in manufacturing. The

Address correspondence to T. J. Burns, NIST, 100 Bureau Drive, Mail Stop 8910, Gaithersburg, Maryland 20899-8910, USA. E-mail: timothy.burns@nist.gov

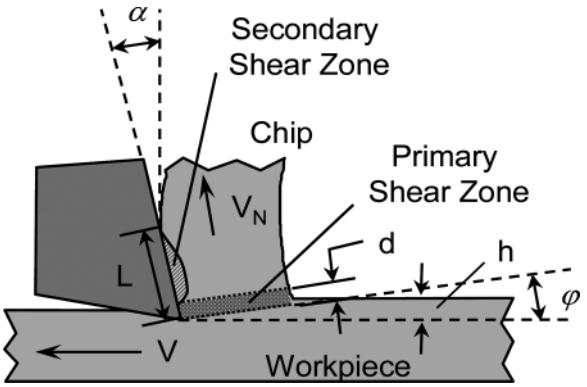

FIGURE 1 Schematic illustration of orthogonal cutting.

fundamental problem that needs to be modeled is chip formation. During chip formation, the work piece interacts with a cutting tool under extreme conditions of pressure and temperature, and large plastic deformation takes place at a very high rate of strain, both in the thin primary shear zone, and in the secondary shear zone along the tool/work interface, as the newly cut material slides up the rake face of the tool (see Figure 1). In some materials, the temperature during high-speed cutting can rise to a significant percentage of the melting temperature (Trent and Wright, 2000; Tlusty, 2000; Davies et al., 2003a; Davies et al., 2003b).

Even though great strides have been made in modeling and simulation capabilities in the last few decades, due in large part to the development of user friendly finite element software packages, such as Abaqus (Simulia), DEFORM (Scientific Forming Technologies), and AdvantEdge (Third Wave Systems), there continues to be a need for higher precision and reliability in the modeling and simulation of machining processes (Ivester et al., 2000; Davies et al., 2000; Arrazola, 2003; Ivester et al., 2007). One of the major challenges to improved modeling and simulation is the determination of an appropriate material description, i.e., constitutive response model, for the flow stress in the workpiece (Childs, 1998; Davies, et al., 2003b; Burns, et al., 2004). In this paper, we provide an update on some ongoing research in the NIST Pulse-Heated Kolsky Bar Laboratory (Mates, et al., 2008), an experimental facility which has been developed for obtaining constitutive response data for application to machining studies as well as for other applications.

In what follows, we begin by reviewing an example of orthogonal cutting considered by Tlusty (2000), in order to emphasize just how extreme the plastic deformation conditions are in a routine high-speed machining operation. Next, we discuss the limitations on reproducing machining conditions by current material testing capabilities. Following this discussion, we provide a brief description of the current status of our Kolsky Bar Laboratory, with an

emphasis on its unique pulse-heating capabilities for rapidly pre-heating a sample, and then holding it at a prescribed temperature for up to several seconds, prior to performing a compression test. In addition, we outline some of our current experimental work in the laboratory that is aimed at providing improved stress-strain data for machining applications. This research program is based on a combination of pulse heating, followed by impact testing, and finally by post-test metallurgical analysis of a sample.

After this introductory and background discussion, we present the results of some recent experiments we have performed on AISI 1075 steel, as part of some ongoing research on the dependence of the flow stress in carbon steels upon the heating rate and time at temperature of the material. We show that, as the result of a phase transformation from the stronger bcc pearlitic structure to a structure that includes less-strong fcc austentite under pulse-heating conditions, there is a decrease in flow stress by approximately 50%.

Although carbon steels with a smaller percentage of carbon, such as AISI 1045, are used much more frequently than a spring steel like AISI 1075 in manufacturing processes that involve high-speed machining operations, AISI 1075 was chosen for this study, because it has the lowest austenization temperature among the carbon steels; see Figure 2. As far as we

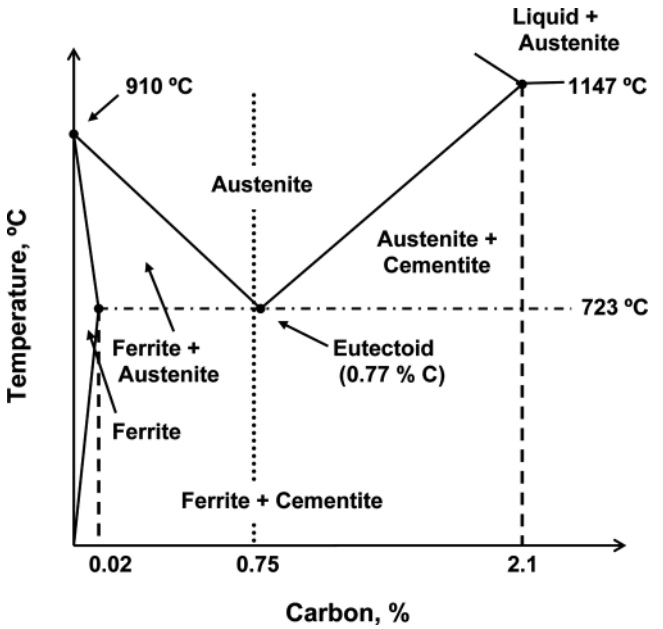

FIGURE 2 Schematic drawing of equilibrium iron-carbon phase diagram for carbon percentages and temperatures of interest in this study. Dotted vertical line at 0.75% carbon is close to the eutectoid composition at 0.77% carbon.

have been able to determine, no high-strain-rate, high-temperature constitutive data have been published for this material; however, Sandvik (1996) gives a specific cutting force of 2239 N/mm^2 for unalloyed carbon steel with a carbon content of less than 0.8%. The AISI 1075 test samples used in this study were carefully heat treated prior to testing, so that they had a uniform pearlitic microstructure. Although the primary goal of the work presented here was not to develop a specific constitutive response model for AISI 1075, we discuss the challenge that the data given in this paper pose for the development of a conventional fixed-parameter constitutive model, like that of Johnson and Cook (1983), for the flow stress of this material.

CHIP FORMATION

Orthogonal Machining of Carbon Steel

Following Tlusty (2000), consider chip formation during orthogonal machining of AISI 1035 steel, with the following parameters: uncut chip thickness $h = 0.2\,\text{mm}$, chip width $b = 6\,\text{mm}$, shear zone thickness $d = 0.02\,\text{mm}$, cutting speed $V = 3\,\text{m/s}$, rake angle $\alpha = 10^\circ$, and shear plane angle $\varphi = 28^\circ$ (see Figure 1). Because plastic deformation in non-porous metals conserves volume, the normal speed of the work material as it flows through the primary shear zone has the constant value $V_N = V\sin(\varphi) = 1.41\,\text{m/s}$. The corresponding shearing speed of the material entering the primary shear zone is given by $V_S = V cos(\varphi)/cos(\varphi - \alpha) = 3.11\,\text{m/s}$. The corresponding chip speed, which is the speed at which the chip moves relative to the tool along the tool face, can be shown to be $V_C = V\sin(\varphi)/\cos(\varphi - \alpha) = 1.48\,\text{m/s}$. Note that V_N and V_C differ only by about 5% in this example.

Using a method due to Piispanen (1948), the shear strain in the primary shear zone may be estimated by $\gamma = V_S/V_N = \cos(\alpha)/[\sin(\varphi)\ \cos(\varphi - \alpha)] = 221\%$, which is very large. The corresponding average shear strain rate can then be estimated by $\dot{\gamma} = \gamma/\Delta t_1$, where $\Delta t_1 = d/V_N = 1.42 \times 10^{-5}\,\text{s}$ is the time interval required to deform an element of the work material into a corresponding element of the chip; this gives $\dot{\gamma} = 1.56 \times 10^5\,\text{s}^{-1}$, which is also very large. At the slower cutting speed of 2 m/s, Tlusty estimates the temperature near the chip/tool interface to be about 900°C. This is consistent with the temperature measured in AISI 1045 steel at 3.2 m/s by Davies et al. (2003a). The chip remains in contact with the tool over a contact length that we estimate, following Tlusty again, to be four times the undeformed chip thickness, $L = 4h = 0.8\,\text{mm}$, so that $d \ll L$. If the uncut material entering the primary shear zone is at room temperature $T_0 = 25^\circ\text{C}$, this gives a huge thermal gradient of approximately $(900 - T_0)/L = 1.09 \times 10^6\,^\circ\text{Cm}^{-1}$. If we estimate the time required for the deformation in the

secondary shear zone to take place by $\Delta t_2 = L/V_C$, then $\Delta t_2 = 5.41 \times 10^{-4}$ s. Using Δt_2 as an estimate of the time required to heat the work material from room temperature up to the maximum temperature, this gives an average heating rate of $(900 - T_0)/\Delta t_2 = 1.62 \times 10^6\,^{\circ}\mathrm{C\,s^{-1}}$, which is also very high.

Constitutive Response Data

Ideally, a carefully designed orthogonal cutting operation could be used for the determination of material constitutive properties for the modeling of machining processes. During continuous chip formation, the process is steady state, and the strain, strain rate, and temperature are of the correct orders of magnitude for machining. Although considerable progress has been made in the measurement of aspects of orthogonal metal cutting, the best attempts to date to identify constitutive parameters using this method still require a considerable amount of analytical modeling; see, e.g., (Tounsi et al., 2002; Özel and Zeren, 2006). Thus, this approach cannot yet be viewed entirely as one of making improved experimental measurements. There are also questions about the uniqueness of the constitutive model parameters that are obtained from cutting experiments (Özel, 1998).

The most common experimental method that is currently used for obtaining constitutive response data for finite-element modeling of machining, as well as for more general purposes, is the split-Hopkinson pressure bar (SHPB) (Gray, 2000). This instrument is also known as the Kolsky bar, after the man who made a number of improvements to Hopkinson's experimental design (Kolsky, 1949). Using this method, the constitutive response data required for the deformation processes modeled by these sophisticated software packages are obtained under conditions that do not approach those that occur during high-speed machining; see, e.g., Jaspers and Dautzenberg (2002a, 2002b).

In particular, the maximum strain rates that are typically attained in a Kolsky bar test are $\sim 1 \times 10^4\,\mathrm{s^{-1}}$. There are also methods for loading the sample in tension (Nicholas, 1981) and in torsion (Hartley et al., 1985), to approximately the same strain rates, on the Kolsky bar. Typical maximum strains obtained with a compressional Kolsky bar are ~50%; larger strains, ~1, can be obtained with the torsional bar test. Thus, with these methods, the strain rate is an order of magnitude smaller than is routinely observed in high-speed machining. Additionally, when the influence of thermal softening on material strength is measured during a Kolsky bar test, the traditional method, in the case of the compression test, is to preheat the sample slowly in situ, followed by dynamic loading of the sample. This

heating method also preheats the sections of the elastic bars adjacent to the sample, which limits the maximum attainable sample temperature and complicates the data analysis (Sharpe, 2008).

Improvements in the heating rate and the attainable uniform sample temperature prior to testing in a Kolsky bar have been made. An induction method has been developed for in situ pre-heating in the dynamic tensile test (Rosenberg et al., 1986). Frantz, et al. (1984) have developed a method for pre-heating the sample in situ using a furnace, and then rapidly bringing the pressure bars into contact with the sample, prior to the dynamic compression test (also see Jaspers and Dautzenberg (2002b) and Nemat-Nasser (2009)). In the next section, a description is given of our own method of in situ resistive pre-heating in the compression test (Mates et al., 2008).

Nevertheless, as far as we know, there is currently no experimental method that can simultaneously produce the high heating rates and high temperature conditions that frequently occur during modern machining operations, and also accurately measure the dynamic stress-strain response of a material. It follows that when constitutive models fit with these data are used to predict material response for machining simulations, the results of these calculations are subject to the criticism that they are based on extrapolations to much larger strains, strain rates, and heating rates, and much smaller times at high temperature, than the experimental data on which the models are based. Thus, there is still a considerable need for improvements in experimental methods for the determination of constitutive response data for the modeling and simulation of high-speed machining operations (Ivester et al., 2000).

THE NIST KOLSKY BAR LABORATORY

Split-Hopkinson Pressure Bar

The NIST Kolsky Bar is a precision engineered split-Hopkinson pressure bar (Rhorer et al., 2002). Two high strength maraging steel bars, each of 1.5 m length and 15 mm diameter, are mounted on bearings to enable easy sliding of the bars in the axial direction and to resist bending in other directions. A cylindrical sample of the material to be tested is inserted between the two long bars, carefully aligned for axial symmetry, so that, ignoring radial effects, the data can be analyzed using one-dimensional wave theory. One of the long bars, called the incident bar, is impacted by a striker, launched by an air gun. The striker is a much shorter bar made from the same maraging steel, with the same diameter, as the two long bars.

In this way, the sample is rapidly loaded by a compressive wave. Because there is an impedance mismatch at the sample, and because the system can be modeled fairly accurately by one-dimensional linear elastic wave theory, when the compressive wave arrives at the bar/sample interface, the difference in impedance between the bar and the sample results in a splitting of the input wave into a tensile wave that is reflected back into the incident bar, and a wave that compresses the smaller-diameter sample sufficiently so that it is rapidly and permanently deformed plastically. This compressive wave then propagates into the second long bar, called the transmitted bar. The system is designed so that the only plastic deformation that occurs is in the sample. By means of strain gauges mounted at the midpoints of the input and transmitted bars and one-dimensional elastic wave analysis, the stress vs. strain response of the sample can be obtained.

Subsecond Thermophysics Laboratory

What makes the NIST apparatus unique is the fact that it has been combined with an existing controlled resistive-heating facility, the NIST Subsecond Thermophysics Laboratory (Basak et al., 2004). This laboratory was originally developed to measure physical properties of metals at high temperature, such as the critical point at melting of a pure metal, using rapid resistive heating and non-contact thermometry. It has the capability to pre-heat an experimental sample extremely rapidly, in situ, using precisely controlled DC electrical current.

Combined Pulse-Heated Kolsky Bar Apparatus

To combine the two systems, non-conducting (Delrin® acetal plastic) bearings are used to support the two long bars, with the exception of the bearing at the support at the end of each bar nearest to the sample. At these two interior supports, custom-made graphite-lined metal sleeves are used. Heavy-duty welding cables connect the interior pair of support posts to the DC electrical circuit. The interior support posts are isolated electrically from the surrounding support structure. By means of this design, the incident and transmitted bars can be used to conduct a rapid, controlled DC pulsed electric current of up to several hundred amperes through a metal Kolsky bar sample; see Figure 3. The typical sample size that we use in this system is 2 mm thick and 4 mm in diameter, which is smaller than usual for a 15 mm diameter Kolsky bar system. The reason for using this smaller size is to guarantee that the sample will heat up

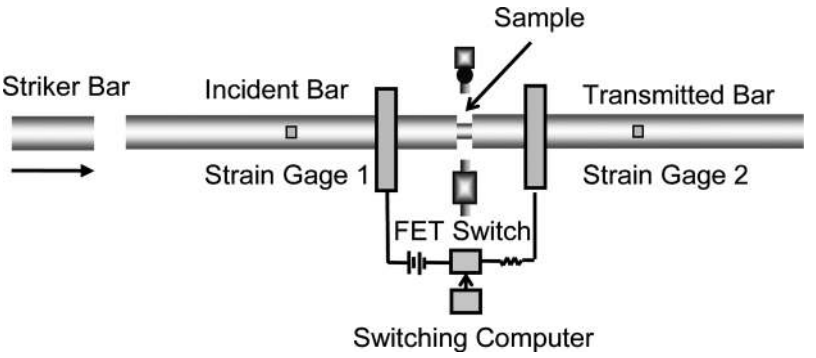

FIGURE 3 Schematic drawing of the NIST Kolsky Bar with DC current pulse-heating capability.

much more rapidly than the interior ends of the two long elastic bars during a test.

The sample temperature is controlled by means of a fast-response pyrometer. The signal from the pyrometer is used to pulse the heating current with sufficient rapidity that the sample quickly reaches and maintains a pre-selected temperature. Using this method, a sample temperature uniformity of 20°C or less can be obtained (Mates et al., 2008). The thermal control system shuts off the DC current within a few milliseconds prior to firing the air gun to launch the striker bar into the incident bar. Once the test is over, the sample typically remains compressed between the bars, and it cools rapidly.

By combining the thermophysics laboratory with a Kolsky bar, we now have a facility for high-strain-rate testing of metal samples that have been pulse-heated prior to stress loading. With the heating rates and temperature control capabilities of this system, together with non-contact thermal measurements, a uniform temperature can reliably be introduced into a sample extremely rapidly. In its present configuration, the NIST Kolsky Bar facility can measure the flow stress of metals at heating rates of up to $6 \times 10^3\,^{\circ}\mathrm{C\,s^{-1}}$. While this heating rate is still orders of magnitude smaller than the $\sim 1 \times 10^6\,^{\circ}\mathrm{C\,s^{-1}}$ that is routinely observed in high-speed machining processes, as discussed in the example in the preceding section, it is much more rapid than the rates at which material samples are pre-heated using more traditional methods.

In the next section, new data are presented from a sequence of pulse-heated high-strain-rate Kolsky bar experiments that were performed on AISI 1075 steel at temperatures that were both below and above the austenite formation temperature, 723°C. As discussed previously, this is certainly within the minimum and maximum range of temperatures that routinely occur during high-speed machining of carbon steels.

APPLICATION TO AISI 1075 STEEL

Discussion of Microstructure

During a high-speed machining operation on a carbon steel, the material undergoes rapid heating. Furthermore, because the resulting chip is quickly exposed to air or to a cooling fluid, upon separation from the tool, the work material is rapidly quenched. It follows that it undergoes a rapid heating-cooling cycle, much like a pulse-heated Kolsky bar sample. Although the Kolsky bar heating rate is not as rapid as in machining, it is still fast enough to study some interesting dependence of the flow stress on the rate of heating and the time at temperature.

At room temperature, an iron-carbon alloy such as AISI 1075 is typically a solid mixture of two body-centered-cubic (bcc) crystalline materials, ferrite (iron) and cementite (iron carbide) (Thelning, 1984). The steel used in our tests was heat treated to obtain a uniform initial microstructure of 100% fine pearlite. In this microstructure, the ferrite and cementite particles form into thin lamellae, or plates, which alternate within the structure; see Figure 4. With 0.75% carbon content, AISI 1075 steel is near the eutectoid composition (0.77% carbon), and its eutectoid temperature is close to 723°C, which is the lowest among the carbon steels (Figure 2).

When heated to a temperature exceeding the eutectoid temperature, and then maintained isothermally, pearlite undergoes a phase transformation into homogeneous austenite, a face-centered cubic solid solution, also called the γ-phase, which is unstable at temperatures below the eutectoid. This phase transformation results from the diffusion of carbon into solid solution with the iron. What this means from the point of view of the present discussion is that, under isothermal heating conditions, this

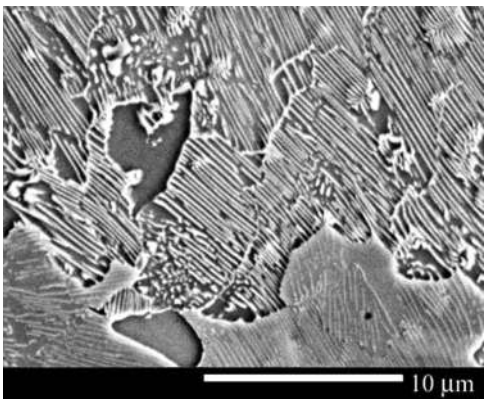

FIGURE 4 AISI 1075 samples were heat-treated to obtain a uniform, nearly 100% fine pearlitic microstructure prior to testing.

material transforms to austenite (100% γ-phase), a face-centered-cubic structure (fcc), at the lowest temperature of the carbon steels. Because of this property, due to its location on the iron-carbon phase diagram, this particular alloy enables a measurement to be made most easily of the strength difference that occurs in a carbon steel as a result of the transformation from one single-phase bcc material (pearlite) that is very strong, to another single phase fcc material (austenite) that is less strong.

As with all diffusion processes, a sufficient amount of time is required for equilibrium to be attained. If the time at temperature is too short, the original pearlite will not have enough time to transform into austenite. As the time at temperature increases, an increasing percentage of the pearlite will transform into austenite, so that there will be a non-equilibrium solid solution consisting partially of austenite. When austenite is cooled very rapidly, i.e., quenched, to room temperature, it transforms into martensite. Martensite consists of fine, irregular plate-like crystals having the composition of the austenite from which it formed. Since martensite cannot form from quenched pearlite, the appearance of martensite in a tested sample indicates that it had undergone austenitization prior to quenching. Thus, by using metallurgical techniques to measure the percentage of martensite in the material after a rapid heating-cooling cycle, the percentage of austenite that was present during the rapid heating phase can be determined.

Kolsky Bar Data

As has already been discussed above, the samples were heat treated prior to testing, so that the initial microstructure was uniformly fine pearlitic; see Figure 4. This was done in order to guarantee that any loss of strength due to austenitization would be a maximum, because we were unsure of what the magnitude of this difference in measured flow stress would be. We are unaware of any published estimates of this strength difference in a carbon steel that depends upon on the heating rate and the time at temperature of the test material.

A series of Kolsky bar tests were performed on samples of this heat-treated AISI 1075 steel, at room temperature and also on pulse-heated samples. The flow stress and the true strain rate measured in one of the room-temperature tests are shown in Figure 5. In the pulse-heated tests, the sample was heated to the test temperature within approximately 1.5 seconds in two stages, and then it was held at temperature for approximately an additional 3.5 seconds, before the compression wave reached the sample.

A typical heating history is shown in Figure 6. The sample temperature is controlled using a millisecond resolution Near Infrared Micro PYrometer

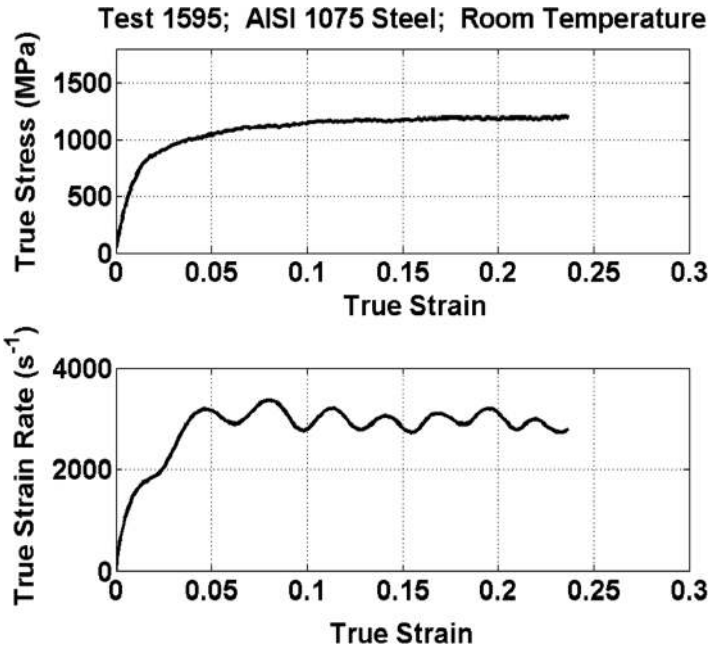

FIGURE 5 Results of Kolsky bar test on a room-temperature sample of AISI 1075 steel. True stress at 10% true strain is approximately 1140 MPa; true strain rate is approximately $3500\,s^{-1}$.

(NIMPY) that serves as a feedback sensor for the DC power supply. The NIMPY is not operational below 300°C. To avoid problems with electrical arcing, the samples were first heated with a lower current to an intermediate temperature that was much less than the eutectoid temperature, in a time on the order of 1 s. During the second heating stage, the samples were heated to the final test temperature at a rate of about $1000°C\,s^{-1}$. The current was then shut off, and the samples were mechanically deformed to a true strain on the order of 25%–35% within the next 100 μs; see Mates et al. (2008) for more details on the sample pre-heating system. The true strain rate in all of these tests was approximately $3500\,s^{-1}$. After the sample was compressed, the cooling rate in our experiments, as determined from the thermocouple cooling history, was approximately $500°C\,s^{-1}$.

Pulse-heated compression tests were performed at temperatures both considerably below and above the eutectoid temperature, and also at a sequence of temperatures at smaller increments on either side of the transition temperature. Thus, the initial sample pre-heating state could be visualized as a point on the dotted vertical line in Figure 2. It is less easy to summarize the states of all of the samples after first pre-heating and then rapidly compressing them. In Figure 7, the flow stress at 10% true strain vs. the measured test temperature of each pulse-heated sample is plotted. The

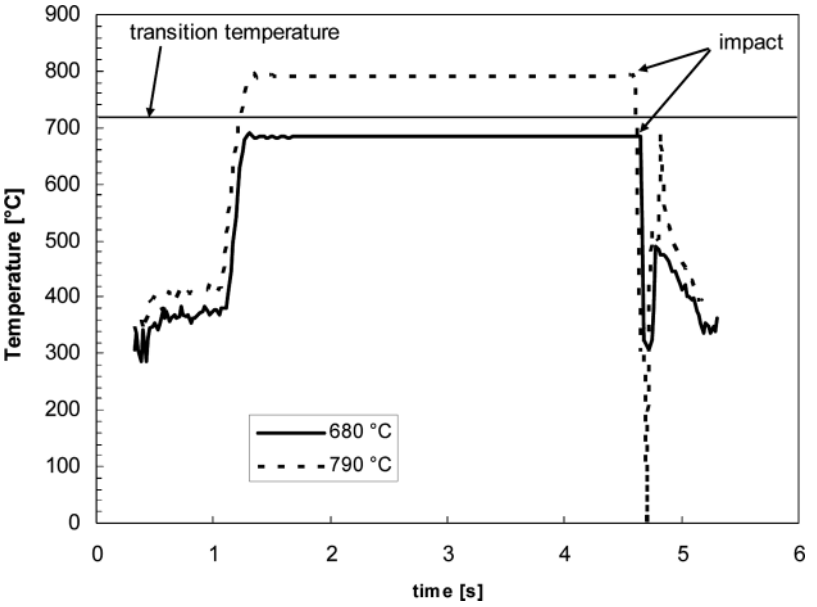

FIGURE 6 Example temperature histories of test samples pulse-heated to below (solid curve) and above (dashed curve) the transition temperature prior to a high strain rate compression test. The sample temperature is controlled using a millisecond resolution Near Infrared Micro PYrometer (NIMPY) that serves as a feedback sensor for the DC power supply; the NIMPY is not operational below 300°C. The samples were first heated with a lower current to an intermediate temperature that was much less than the eutectoid temperature, in a time on the order of 1 s. They were then heated to the test temperature in a faster second stage, at a rate of about $1000°C\,s^{-1}$.

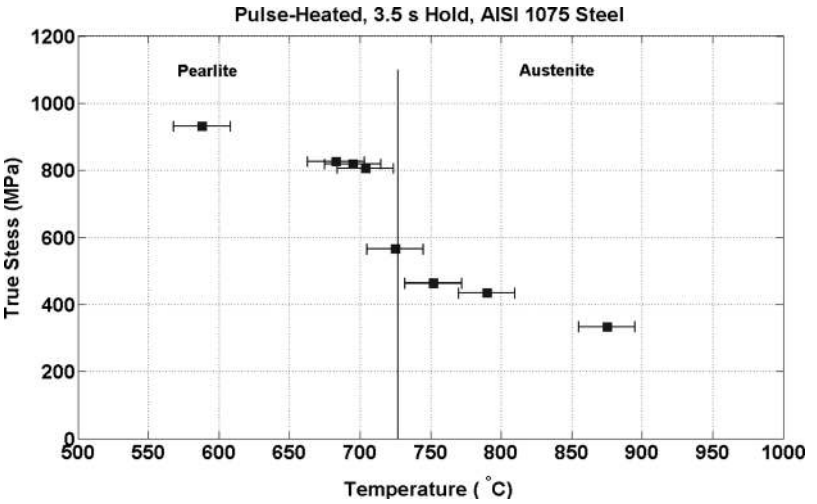

FIGURE 7 Kolsky bar experimental data on AISI 1075 steel; pearlitic room-temperature samples were pulse-heated and then held at temperature for 3.5 s; vertical line denotes the eutectoid temperature (723°C); squares denote the flow stress at 10% true strain, $\sim 3500\,s^{-1}$ true strain rate; error bars denote 2σ.

error bars denote the 2σ uncertainty in the temperature measurements. The 2σ uncertainty in the stress measurements was estimated to be no more than 5%; for this reason, these error bars were not plotted, since there was much more uncertainty in the temperature measurements. The random error propagation techniques that were used to estimate these measurement uncertainties may be found in Mates et al. (2008).

The experimental data show that across the transition temperature, there is a reduction in flow stress of about 50%. A metallurgical analysis was performed on the post-test samples, in order to correlate the microstructure of the material with the measured flow stress. The results indicated that, in all of the tests conducted at temperatures that were at least several degrees above the transition temperature (723°C), the post-test sample microstructures were fully martensitic with no trace of retained pearlite, indicating that a complete transformation had occurred in these tests; see Figure 8.

On the other hand, all of the samples that had been pre-heated to temperatures below the transition temperature contained untransformed pearlite, indicating that no transition took place in these tests; see Figure 9. In a test in which the sample had been pre-heated to a temperature of 725°C, which is very close to the transition temperature, the post-test metallurgical analysis showed an altered coarsened pearlitic structure. In this test, the sample failed to quench rapidly enough to form martensite, meaning that it was difficult to tell whether austenite, pearlite, or a mixture of the two phases was present when the compression test occurred; see Figure 10. However, the magnitude of the flow stress in this test indicated that most of the pearlite had transformed into austenite. In the next

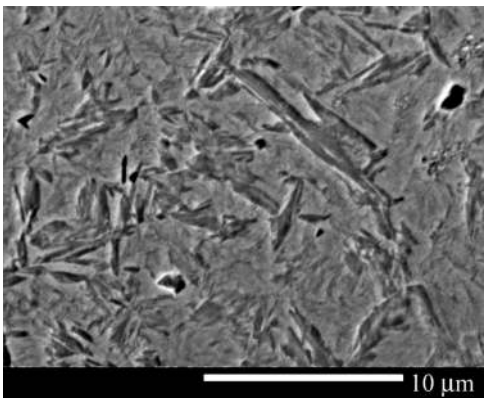

FIGURE 8 AISI 1075 test sample that was pulse-heated to 752°C, and then rapidly compressed in a Kolsky bar apparatus. The microstructure is fully martensitic, with no trace of retained pearlite, indicating that a complete transformation from pearlite to austenite had occurred prior to the compression test.

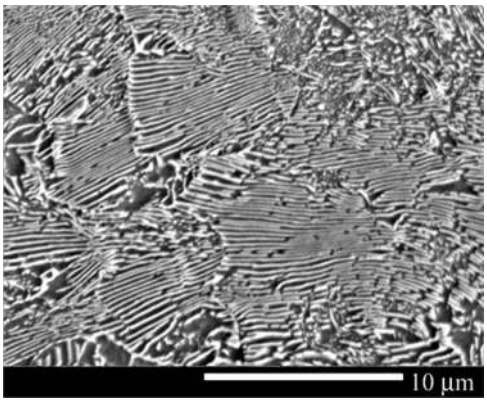

FIGURE 9 AISI 1075 test sample that was pulse-heated to 588°C, and then rapidly compressed in a Kolsky bar apparatus; the microstructure is still fine pearlitic, indicating that no transition to austenite occurred during the test.

section, the implications of the test results presented in Figure 7 for the constitutive response modeling of AISI 1075 are discussed.

CONSTITUTIVE MODELING OF AISI 1075 DATA

Johnson-Cook Flow Stress Model

The Johnson-Cook flow stress model (Johnson and Cook, 1983) is a commonly used constitutive response function for finite-element

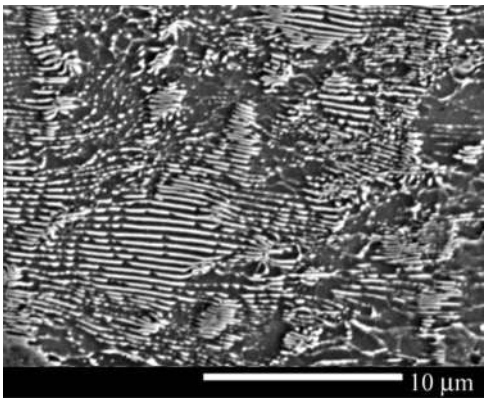

FIGURE 10 AISI 1075 test sample that was pulse-heated to 725°C, and then rapidly compressed in a Kolsky bar apparatus. Post-test metallurgical analysis showed an altered coarsened pearlitic structure. In this test, the sample failed to quench rapidly enough to form martensite, meaning that it was difficult to tell whether austenite, pearlite, or a mixture of the two phases was present when the compression test occurred to austenite.

simulations of the rapid plastic deformation of metals; see, e.g., Meyers (1994); Jaspers and Dautzenberg (2002b). This phenomenological model expresses the von Mises flow stress, σ as a function of the true strain, true strain rate, and temperature,

$$\sigma = [A + B\bar{\varepsilon}^n]\left[1 + C\ \ln \dot{\bar{\varepsilon}}^*\right][1 - (T^*)^m]. \tag{1}$$

In Equation 1, $\bar{\varepsilon}$ is the equivalent plastic strain, $\dot{\bar{\varepsilon}}^* = \dot{\bar{\varepsilon}}/\dot{\bar{\varepsilon}}_0$ is the dimensionless true strain rate, $\dot{\bar{\varepsilon}}_0 = 1.0\,\mathrm{s}^{-1}$, and T^* is the homologous temperature, a dimensionless quantity that is defined as follows,

$$T^* = \frac{T - T_0}{T_M - T_0}. \tag{2}$$

Here, T is the temperature in degrees C, $T_0 = 20°\mathrm{C}$ is the initial temperature, and T_M is the melting temperature of the material. A, B, C, n, and m are five material constants that are fit to experimental data. Note that Equation 1 is a product of three power-law expressions, with each term involving only one of the independent variables.

The purely empirical Johnson-Cook model for a specific material is usually determined in three steps; see, e.g., Meyers (1994). First, the parameters in the leading term are determined using quasi-static tension or torsion data; A is the yield strength of the material, and B and n estimate its strain-hardening behavior. Second, the thermal softening fraction K_T is determined by computing the ratio of the stress in a heated test to that in a room-temperature test at the same strain rate. It then follows that

$$m = \ln\,(1 - K_T)/\ln\,T^*. \tag{3}$$

In the third step, the strain-rate sensitivity coefficient C is determined by using the flow stress values at a fixed strain from two different room temperature tests, performed at two different strain rates. Some authors use optimization methods to determine the best-fit parameter values for sets of data on a given material that have been measured experimentally; see, e.g., Milani, et al. (2006).

Application to AISI 1075 Data

Now, consider the AISI 1075 data given in Figure 7. All of these experiments were performed at a nominal strain rate of approximately $3500\,\mathrm{s}^{-1}$. Therefore, if we assume that the top curve of the high strain-rate room temperature test has been well-fit by finding the coefficients A, B, C, and n in Equation 1, it follows that the flow stress at 10% strain and $3500\,\mathrm{s}^{-1}$ will

approximately be equal to 1140 MPa. Keeping the strain fixed at 10% and the strain rate fixed at 3500 s^{-1}, Equation 1 can be written as

$$\sigma = [1 - (T^*)^m] \times 1140\,\text{MPa}. \tag{4}$$

In Figure 11, the isolated circle at $T_0 = 25°C$ and $\sigma = 1140$ MPa is the flow stress at $T = T_0$, so that $T^* = 0$. The pulse-heated data at 10% strain given in Figure 7 are also re-plotted in Figure 11. Using the cold flow stress at T_0 as the initial point, and fixing the melting temperature at $T_M = 1516°C$ in Equation 2, Equation 4 is plotted in Figure 11 with $m = 1.6$ (upper curve), $m = 1.0$ (center line), and $m = 0.7$ (lower curve) on the temperature interval [T_0, 1000°C].

A number of conclusions can be drawn from Figure 11. With the thermal-softening parameter value $m = 1.6$, Equation 4 predicts the flow stress fairly well at elevated temperatures that are below 723°C. On the other hand, using the thermal parameter value $m = 0.7$, Equation 4 predicts the flow stress values above 723°C fairly well. This is why these two values of m were chosen. However, for the carbon steels AISI 1006 and AISI 1045, it has been found from experimental data on slowly pre-heated samples by a number of authors that the thermal parameter $m \approx 1.0$ (Johnson and Cook,

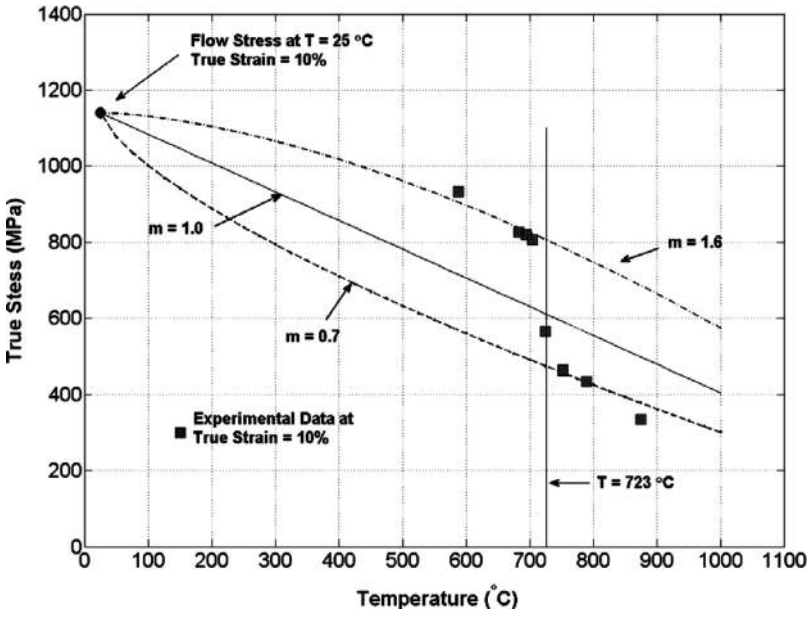

FIGURE 11 Flow stress at 10% true strain. Upper (dash-dot) curve: $m = 1.6$; middle (solid) curve: $m = 1.0$; lower (dash) curve: m=0.7. Vertical line denotes eutectoid temperature. Circle is experimental data from room temperature test; squares are experimental data from tests in which sample was pulse-heated and then held at constant temperature for ~3.5 s before impact.

1983; Meyers, 1994; Jaspers and Dautzenberg, 2002b; Özel and Karpat, 2007). Use of $m=1$ in Equation 4 provides a poor prediction for all but one of the pulse-heated data points. Overall, the Johnson-Cook model with constant m does a poor job of fitting all of the data in Figure 11, where evidently there is a phase transition in the microstructure at the eutectoid temperature from a pearlite to austenite.

DISCUSSION AND CONCLUDING REMARKS

We have presented new experimental results on pulse-heated AISI 1075 steel. These data were shown to present a constitutive modeling challenge, because of a phase transformation from pearlite to austenite that took place in the material microstructure when the sample was rapidly pre-heated to a temperature above 723°C prior to rapid compression testing. In an experimental study of austenite formation in 0.75% carbon steel using dilatometry, Rose and Strassburg (1956) and Thelning (1984) have published heating time-temperature transformation (TTT) curves that indicate that a time of 3.5 seconds at high temperature is insufficient for the transformation to austenite to run to completion. Based on this, we expected that a flow stress-temperature curve like the upper curve in Figure 11 with $m>1$ would fit our experimental data on pulse-heated AISI 1075 fairly well. However, this is clearly not the case. Therefore, the data presented here are very interesting, because they show that there is indeed evidence of the phase transformation, even for this relatively short time at high temperature.

We are unaware of any studies that have attempted to measure strength differences that may occur in a carbon steel as the result of phase transformations under the conditions of simultaneous very rapid heating and compression that occur during high-speed machining. Although our experimental work involves pre-heating a sample prior to loading it, we believe that the new constitutive response data presented in this paper may help to explain why the results of many finite-element simulations of high-speed machining operations, while providing much useful insight into the physics of these operations, often fail to give good predictions of essential quantities such as forces and temperatures; see, e.g., Arrazola (2003).

As already mentioned, carbon steels with a smaller percentage of carbon, such as AISI 1045, are of much more interest than AISI 1075 for the modeling and simulation of manufacturing processes that involve high-speed machining operations. For this reason, no attempt was made to construct a complete constitutive model for AISI 1075 in the present study. However, it would be of great interest to investigate whether or not a series of dynamic pulse-heated tests on samples of AISI 1045 steel,

prepared from commercial bar stock, show a response similar to that described by Equation 4, with $m > 1$ for experiments in which the testing temperature is less than the eutectoid temperature, and $m < 1$ for experiments in which the testing temperature is greater than the eutectoid temperature. This will be the subject of a subsequent paper.

DISCLAIMER

Commercial products are identified in order to specify certain procedures or equipment used. In no case does such identification imply recommendation or endorsement by the National Institute of Standards and Technology, nor does it imply that the identified products are necessarily the best available for the purpose.

NOMENCLATURE

h	chip thickness
b	chip width
d	shear zone thickness
V	cutting speed
α	rake angle
φ	shear plane angle
V_N	work material speed normal to primary shear zone
V_S	shearing speed of work material in direction of primary shear zone
V_C	chip speed speed parallel to the face of the tool
γ	shear strain
$\dot{\gamma}$	shear strain rate
Δt_1	time work material spends in primary shear zone
L	contact length of chip along face of tool
Δt_2	time work material spends in secondary shear zone
σ	von Mises flow stress
$\bar{\varepsilon}$	equivalent plastic strain
$\dot{\bar{\varepsilon}}^*$	dimensionless true strain rate
$\dot{\bar{\varepsilon}}_0$	reference strain rate for non-dimensionalization
T^*	homologous temperature
T	temperature
T_0	initial temperature
T_{M}	melting temperature
A,B,C,m,n	Johnson-Cook empirical material constants

REFERENCES

Arrazola, P.-J. (2003) *Modélisation numérique de la coupe: Etude de sensibilité des paramètres d'entrée et identification du frottement entre outil-copeau*, Phd. Thesis, E.C. Nantes, France.

Basak, D.; Yoon, H.W.; Rhorer, R.; Burns, T.J.; Matsumoto, T. (2004) Temperature control of pulse heated specimens in a Kolsky bar apparatus using microsecond time-resolved pyrometry. *International Journal of Thermophysics*, 25(2): 561–574.

Burns, T.J.; Davies, M.A.; Rhorer, R.L.; Basak, D.; Yoon, H.W.; Fields, R.J.; Levine, L.E.; Cao, Q.; Cooke, A.L.; Whitenton, E.P.; Kennedy, M.D.; Ivester, R. (2004) Influence of heating rate on flow stress in high-speed machining processes. In *Proceedings of the 7th CIRP International Workshop on Modeling of Machining Operations*, Cluny, France.

Childs, T.H.C. (1998) Material property needs in modeling metal machining. *Journal of Machining Science and Technology*, 2(2): 303–316.

Davies, M.A.; Yoon, H.; Schmitz, T.L.; Burns, T.J.; Kennedy, M.D. (2003a) Calibrated thermal microscopy of the tool-chip interface in machining. *Journal of Machining Science and Technology*, 7(2): 166–190.

Davies, M.A.; Cao, Q.; Cooke, A.L.; Ivester, R. (2003b) On the measurement and prediction of temperature fields in machining AISI 1045 steel. *Annals of the CIRP*, 52(1): 77–80.

Frantz, C.E.; Follansbee, P.S.; Wright, W.T. (1984) Experimental techniques with the split Hopkinson pressure bar. In *High Energy Rate Forming*; Berman, I.; Schroeder, J.W. (Eds.), ASME: New York, pp. 229–236.

Gray, G.T. III (2000) Classic split-Hopkinson pressure bar testing. In *Metals Handbook* 10th Edition, American Society of Metals: Materials Park, Ohio, Volume 8, pp. 462–476.

Hartley, K.A.; Duffy, J.; Hawley, R.E. (1985) The torsional Kolsky (split-Hopkinson) bar. In *Metals Handbook*. 9th Edition, American Society of Metals: Materials Park, Ohio, Volume 8, pp. 218–228.

Ivester, R.; Kennedy, M.; Davies, M.; Stevenson, R.; Thiele, J.; Furness, R.; Athavale, S. (2000) Assessment of machining models: Progress report. *Journal of Machining Science and Technology*, 4(3): 511–538.

Ivester, R.; Whitenton, E.; Heigel, J.; Marusich, T.; Arthur, C. (2007) Measuring chip segmentation by high-speed microvideography and comparison to finite-element modeling simulations. In *Proceedings of the 10th CIRP International Workshop on Modeling of Machining Operations*, Calabria, Italy..

Jaspers, S.P.F.C.; Dautzenburg, J.H. (2002a) Material behavior in metal cutting: Strains, strain rates, and temperatures in metal cutting. *Journal of Materials Processing Technology*, 121: 123–135.

Jaspers, S.P.F.C.; Dautzenburg, J.H. (2002b) Material behavior in conditions similar to metal cutting: flow stress in the primary shear zone. *Journal of Materials Processing Technology*, 122: 322–330.

Johnson, G.J.; Cook, W.H. (1983) A constitutive model and data for metals subjected to large strains, high strain rates, and temperatures. In *Proceedings of the 7th Symposium on Ballistics*, The Hague, pp. 541–547.

Kolsky, H. (1949) An investigation of the mechanical properties of materials at very high rates of loading. *Proceedings of the Physical Society of London*, B62: 676–700.

Mates, S.P.; Rhorer, R.; Whitenton, E.; Burns, T.; Basak, D. (2008) A pulse-heated Kolsky bar technique for measuring flow stress of metals subjected to high loading and heating rates. *Experimental Mechanics*, 48: 799–807.

Meyers, M.A. (1994) *Dynamic Behavior of Materials*. John Wiley & Sons: New York, NY.

Milani, A.S.; Dabboussi, W.; El-Lahham; C.; Nemes J.A.; Aberyaratne, R.C. (2006) On obtaining material parameters for general purpose finite element models. In *Proceedings of the 17th IASTED International Conference on Modelling and Simulation*, Montreal, QC, Canada.

Nemat-Nasser, S. (2009) *Plasticity: A Treatise on Finite Deformation of Heterogeneous Inelastic Materials*. Cambridge University Press: Cambridge, UK.

Nicholas, T. (1981) Tensile testing of materials at high rates of strain. *Experimental Mechanics*, 21: 177–185.

Özel, T. (1988) *Investigation of High Speed Flat End Milling Process*. PhD Dissertation, The Ohio State University, Columbus, Ohio.

Özel, T.; Karpat, Y. (2007) Identification of constitutive material model parameters for high strain rate metal cutting conditions using evolutionary computational algorithms. *Materials and Manufacturing Processes*, 22: 659–667.

Özel T.; Zeren, E. (2006) A methodology to determine work material flow stress and tool-chip interfacial friction properties by using analysis of machining. *ASME Journal of Manufacturing Science and Engineering*, 128: 119–129.

Piispanen, V. (1948) Theory of formation of metal chips. *Journal of Applied Physics*, 19: 876–881.

Rhorer, R.L.; Davies, M.A.; Kennedy, M.D.; Dutterer, B.S.; Burns, T.J. (2002) Construction and alignment of a Kolsky bar apparatus. In *Proceedings of the American Society for Precision Engineering Annual Conference*, St. Louis, MO.

Rose, A.; Strassburg, W. (1956) Darstellung der Austenitbildung untereutektoidischer Stähle in Zeit-Temperatur-Auflösungs-Schaubildern. *Stahl und Eisen*, 76(15): 976–983.

Rosenberg, Z.; Dawicke, D.; Strader, E.; Bless, S.J. (1986) A new technique for heating specimens in split-Hopkinson bar experiments using induction-coil heaters. *Experimental Mechanics*, 26(3): 275–278.

Sandvik (1996) *Modern Metal Cutting – A Practical Handbook*. Sandvik Coromant, Fair Lawn, NJ.

Tlusty, J. (2000) *Manufacturing Processes and Equipment*, Prentice-Hall, Upper Saddle River, NJ.

Tounsi, N.; Vincenti, J.; Otho, A.; Elbestawi, M.A. (2002) From the basic mechanics of orthogonal metal cutting toward the identification of the constitutive equation. *International Journal of Machine Tools and Manufacture*, 43: 1373–1383.

Trent, E.M.; Wright, P.K. (2000) *Metal Cutting*. 4th Edition, Butterworth-Heinemann: Boston, MA.